

Layer-Specific Fine-Tuning for Improved Negation Handling in Medical Vision-Language Models

Ali Abbasi¹ Mehdi Taghipour² Rahmatollah Beheshti¹

Abstract

Negation is a fundamental linguistic operation in clinical reporting, yet vision–language models (VLMs) frequently fail to distinguish affirmative from negated medical statements. To systematically characterize this limitation, we introduce a radiology-specific diagnostic benchmark that evaluates polarity sensitivity under controlled clinical conditions, revealing that common medical VLMs consistently confuse negated and non-negated findings. To enable learning beyond simple condition absence, we further construct a contextual clinical negation dataset that encodes structured claims and supports attribute-level negations involving location and severity. Building on these resources, we propose Negation-Aware Selective Training (NAST), an interpretability-guided adaptation method that uses causal tracing effects (CTEs) to modulate layer-wise gradient updates during fine-tuning. Rather than applying uniform learning rates, NAST scales each layer’s update according to its causal contribution to negation processing, transforming mechanistic interpretability signals into a principled optimization rule. Experiments demonstrate improved discrimination of affirmative and negated clinical statements without degrading general vision–language alignment, highlighting the value of causal interpretability for targeted model adaptation in safety-critical medical settings. Code and resources are available at <https://github.com/healthylife/NAST>.

1. Introduction

Vision–language models (VLMs) have achieved impressive performance across a range of multimodal tasks, including image–text retrieval, visual question answering, and medical

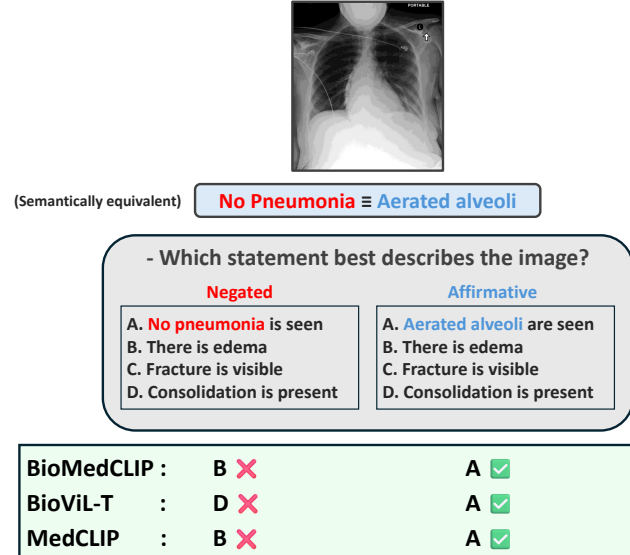


Figure 1. Negation failure under polarity-controlled medical descriptions. For the same chest X-ray, two multiple-choice sets are identical except for a single semantically equivalent phrase: a negated finding (“No pneumonia is seen”) versus its affirmative counterpart (“Aerated alveoli are seen”). Despite the minimal wording change and shared clinical meaning, representative medical VLMs predict correctly under the affirmative phrasing but fail under the negated phrasing, illustrating a systematic affirmative bias.

report understanding (Radford et al., 2021; Li et al., 2022; Alayrac et al., 2022). In clinical settings, such models are increasingly used to associate radiological images with textual descriptions, enabling applications such as automated report generation and decision support (Wang et al., 2022; Zhang et al., 2023b; Lin et al., 2023; Bannur et al., 2023). However, despite strong aggregate performance, recent evidence suggests that VLMs often rely on shallow correlations between visual features and textual tokens, raising concerns about their robustness to linguistically subtle but clinically critical distinctions (Yuksekgonul et al., 2022; Liu et al., 2025).

One such distinction is a surprisingly simple linguistic phenomenon — negation (Vatsa et al., 2025). In radiology reports, negation reverses the clinical interpretation of visual findings. Statements such as “no pleural effusion” or “no

¹University of Delaware ²Cleveland Clinic. Correspondence to: Ali Abbasi <aiai@udel.edu>.

consolidation in the right lower lobe” convey the absence of pathology and directly influence downstream clinical decisions. Confusing negated and affirmative statements can lead to serious misinterpretations, even when the underlying visual evidence is correctly perceived (Ko & Park, 2025). While negation has been studied in natural language processing (Chapman et al., 2001; Daelemans, 2012; Ettinger, 2020), its interaction with multimodal representation learning—particularly in medical VLMs—remains poorly understood (Alhamoud et al., 2025).

Negation is challenging for vision–language models because it requires reasoning about how linguistic modifiers alter visual meaning. Since contrastive pretraining is dominated by affirmative image–caption pairs, descriptions of absence (e.g., “no”, “without”) are relatively underrepresented (Ko & Park, 2025). Although recent work has examined negation in multimodal models (Singh et al., 2024; Cai et al., 2025; Han et al., 2025; Alhamoud et al., 2025), most studies focus on general-domain object presence. In medical imaging, however, negation often targets specific attributes—such as location or severity—rather than existence alone (e.g., “No large pleural effusion” or “Consolidation not in the right lower lobe”). Consequently, negation understanding in medical VLMs remains insufficiently explored despite its clinical importance.

In this work, we first show that well-known medical vision–language models exhibit systematic failures in negation understanding. To isolate this behavior, we introduce a radiology-specific diagnostic benchmark that evaluates polarity sensitivity under tightly controlled clinical conditions. The benchmark constructs paired statements that are identical in structure and differ only in clinical polarity (e.g., “Cardiomegaly is seen” vs. “Normal heart size is seen”). Despite their semantic equivalence, models consistently perform better on affirmative formulations than on their negation-equivalent counterparts, revealing a persistent affirmative bias (Figure 1).

Addressing this limitation requires more than simply adding negated examples, as most prior approaches do (Singh et al., 2024; Ko & Park, 2025; Cai et al., 2025; Han et al., 2025; Alhamoud et al., 2025). In clinical language, negation is often contextual and attribute-specific, targeting not only condition existence but also location or severity (Chapman et al., 2001; Harkema et al., 2009). To model this granularity, we construct a contextual clinical negation dataset based on structured radiological claims (Zhang et al., 2023a). Building on this dataset, we propose Negation-Aware Selective Training (NAST), an interpretability-guided adaptation method for CLIP-based medical VLMs. NAST uses causal tracing to estimate each layer’s contribution to negation processing and scales gradient updates accordingly, assigning larger updates to causally influential layers. Experi-

ments show improved discrimination between affirmative and negated clinical statements without degrading general vision–language alignment.

In particular, this paper makes the following contributions:

- **Diagnostic evaluation of negation in medical VLMs:** We introduce a radiology-specific diagnostic benchmark that isolates polarity sensitivity by constructing tightly controlled affirmative–negated statement pairs, revealing systematic failures and an affirmative bias in well-known medical vision–language models.
- **Contextual clinical negation dataset:** We propose a new fine-tuning dataset based on structured radiological claims that captures attribute-level negation—including location and severity—enabling supervision that reflects how negation is expressed in real clinical reports beyond simple condition absence.
- **Negation-Aware Selective Training (NAST):** We present NAST, an interpretability-guided adaptation method for CLIP-based medical VLMs that uses causal tracing effects to modulate layer-wise gradient updates, allocating learning capacity according to each layer’s causal involvement in negation processing.
- **Empirical validation of interpretability-guided optimization:** We show that NAST improves discrimination between affirmative and negated clinical statements while preserving performance on standard multimodal tasks, demonstrating that mechanistic interpretability can guide effective model adaptation in medical settings.

2. Related Work

2.1. Negation in NLP and Multimodal Models

Negation has long been recognized as a core challenge in natural language understanding, particularly in the clinical domain where correctly interpreting negated findings is critical for safe decision-making. Early NLP work developed rule-based and contextual approaches to detect negated and uncertain medical concepts, demonstrating that negation often operates over specific attributes of a condition rather than indicating its absence (Chapman et al., 2001; Harkema et al., 2009; Daelemans, 2012). Analyses of pretrained language models later revealed that, despite contextual representations, models still struggle with polarity reversals and compositional negation, frequently relying on surface-level lexical cues (Ettinger, 2020; Hosseini et al., 2021; Vatsa et al., 2025).

Recent work has shown that controlled linguistic perturbations can expose systematic failure modes in medical large

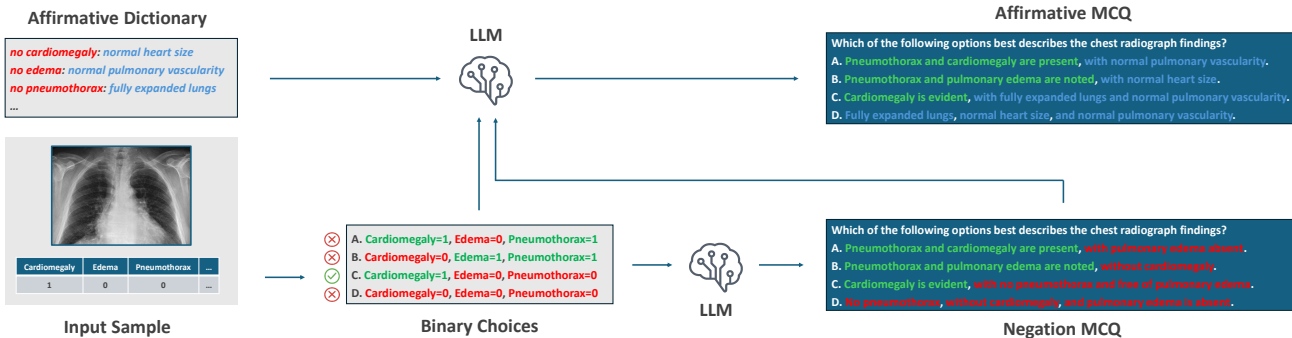


Figure 2. MedNega-CXR benchmark construction pipeline. Starting from MIMIC-CXR images and binary diagnostic labels, the pipeline generates (1) structured label permutations, (2) LLM-generated negation MCQs, (3) affirmative rewrites, and (4) final paired MCQs. All mappings and outputs were reviewed by two board-certified radiologists (10+ years experience).

language models, including shifts in model behavior under counterfactual or minimally modified inputs (Poulain et al., 2024; Fayyaz et al., 2024; Adiba & Beheshti, 2025). More recently, negation has gained attention in multimodal and vision–language learning. Singh et al. introduced CC-Neg and showed that VLMs often fail to associate negated captions with images, motivating contrastive fine-tuning strategies (Singh et al., 2024). Subsequent work proposed multi-level retrieval and multiple-choice diagnostics revealing persistent affirmation bias (Alhamoud et al., 2025), training-time negation generation pipelines (Cai et al., 2025), and test-time adaptation methods addressing distribution shifts between affirmative and negated concepts (Han et al., 2025). In the medical domain, Ko & Park (2025) introduced a negation-aware benchmark and contrastive framework for chest X-ray interpretation.

Despite these advances, existing multimodal negation studies have largely focused on general-domain object absence or data-centric augmentation strategies. Comparatively little attention has been paid to the structured, attribute-level negation that characterizes clinical language, or to how negation is distributed across model layers and learning dynamics.

2.2. Medical Vision–Language Models

Medical vision–language models adapt large-scale multimodal pretraining to the clinical domain by aligning medical images with structured or free-text reports. Early efforts focused on radiology, leveraging paired chest X-rays and reports to learn joint embeddings for retrieval, classification, and report generation. Notable examples include ConVIRT (Zhang et al., 2022) and GLoRIA (Huang et al., 2021), which demonstrated that contrastive pretraining on image–report pairs improves downstream diagnostic performance compared to vision-only models.

Building on CLIP-style architectures (Radford et al., 2021), several works introduced domain-specific adaptations. Med-

CLIP (Wang et al., 2022) replaces web-scale image–text data with curated medical image–report pairs and introduces medical-aware text encoders. BioMedCLIP (Zhang et al., 2023b), PubMedCLIP (Eslami et al., 2023), and PMC-CLIP (Lin et al., 2023) further scale this paradigm by pretraining on large biomedical corpora, including PubMed Central figures and captions, yielding strong zero-shot performance across medical imaging tasks. More recent models such as Med-Flamingo (Moor et al., 2023), UniMed-CLIP (Khattak et al., 2024), and QwenCLIP (Wei et al., 2025), explore instruction tuning and multimodal prompting to better align model outputs with clinical reasoning. However, systematic evaluation of negation handling in medical vision–language models remains limited, highlighting a gap that this work aims to address.

3. A Diagnostic Benchmark for Negation in Medical VLMs

3.1. Motivation

Recent work has begun to benchmark negation understanding in vision–language models through tasks such as image retrieval and multiple-choice question answering (Singh et al., 2024; Alhamoud et al., 2025). While these benchmarks reveal performance gaps between captions that contain negation and those that do not, they typically do not enable direct comparison between negated and affirmative descriptions that convey the same underlying semantic state. As a result, it remains unclear whether observed failures reflect genuine difficulties in reasoning about negation, or broader weaknesses in compositional language–vision alignment.

The medical domain offers a unique opportunity to isolate this phenomenon. Unlike general-domain scenes—where the absence of an object (e.g., “no car”) does not admit a single affirmative equivalent—many negated clinical findings can be naturally expressed using affirmative alternatives

without explicit negation. For example, the absence of pneumonia may be described either as “no pneumonia” or as “aerated lungs.” This property enables controlled evaluation using semantically equivalent sentence pairs that differ only in linguistic polarity.

Motivated by this observation, and by the lack of benchmarks specifically designed to probe negation understanding in medical VLMs, we first construct a diagnostic benchmark that directly contrasts negated and affirmative clinical descriptions under identical visual contexts.

3.2. Benchmark Construction

We build our diagnostic benchmark on CheXpert (Irvin et al., 2019), derived from MIMIC-CXR-JPG (Johnson et al., 2019; Adiba et al., 2026), containing 227,827 studies annotated for 14 radiological conditions with labels: present (1), absent (0), uncertain (−1), or not mentioned. We discard studies labeled *No Finding* and retain those with at least two positive and three absent conditions, ensuring each question includes multiple affirmed findings and at least one negated condition in the correct option. This yields 6,965 samples.

To enable controlled polarity comparisons (i.e., paired descriptions differing only in clinical polarity), we curate affirmative alternatives for each absent condition (e.g., *no cardiomegaly* ↔ *normal heart size*) in consultation with two board-certified radiologists (Appendix A).

For each study, we generate paired multiple-choice questions (MCQs) in three steps: (1) construct contrastive label configurations by permuting condition presence and absence to form hard negatives; (2) use an LLM to generate a radiology-style question with explicit negation; and (3) use a second LLM to produce an affirmative counterpart by replacing negated phrases with curated alternatives while preserving structure.

This yields MCQ pairs differing only in polarity, enabling direct comparison between negated and affirmative formulations. Data are split at the patient level to prevent leakage. Figure 2 illustrates the pipeline; full details appear in Appendix B. The benchmark and generation scripts will be released upon publication.

3.3. Empirical Analysis on Medical VLMs

We evaluate three representative medical vision–language models—BioMedCLIP (Zhang et al., 2023b), BioViL-T (Bannur et al., 2023), and MedCLIP (Wang et al., 2022)—on the proposed benchmark using multiple-choice accuracy, reporting results separately for affirmative and negated MCQ sets (Figure 3). Although the two sets are identical in structure and clinical meaning, all models exhibit a consistent performance gap favoring affirmative formulations.

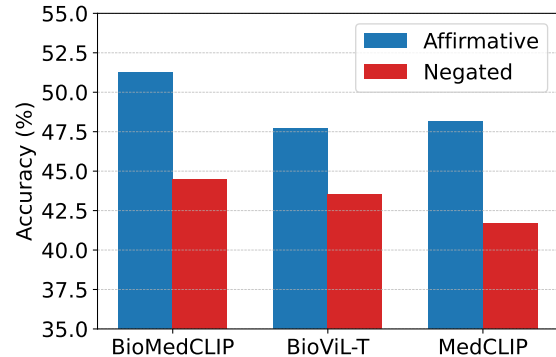


Figure 3. Evaluation of medical vision–language models on the proposed diagnostic benchmark. Accuracy (%) is reported separately for affirmative-equivalent and negated multiple-choice question sets. Despite identical sentence structure and equivalent underlying clinical meaning, all models exhibit consistently lower performance on negated formulations, revealing a systematic affirmative bias in medical VLMs.

This gap persists despite the known difficulty of contrastive models in handling descriptive adjectives and attribute-level semantics (e.g., *normal*, *clear*, *smooth*, *sharp*) (Yuksekgonul et al., 2022; Buettner & Kovashka, 2024). Even though affirmative questions rely on such adjective-based alternatives (Appendix A), models still perform worse on negated formulations, suggesting that the degradation reflects a deeper deficiency in negation sensitivity rather than adjective understanding alone.

4. Method

The results above reveal that medical vision–language models struggle to reliably interpret negated clinical statements, motivating targeted adaptation. We therefore introduce **Negation-Aware Selective Training (NAST)**, a principled fine-tuning framework for CLIP-based medical VLMs. NAST combines a contextual negation dataset with causal tracing to identify layers most influential for negation processing and selectively modulates their updates during training. By grounding optimization in layer-wise causal relevance, NAST improves negation sensitivity while preserving general vision–language alignment.

4.1. Contextual Negation Fine-Tuning Dataset

We construct a large-scale *contextual negation fine-tuning dataset* from MIMIC-CXR (Johnson et al., 2024) using CAD annotations (Zhang et al., 2023a). The approach generalizes to other annotated medical datasets and provides fine-grained, expert-derived supervision for negation understanding.

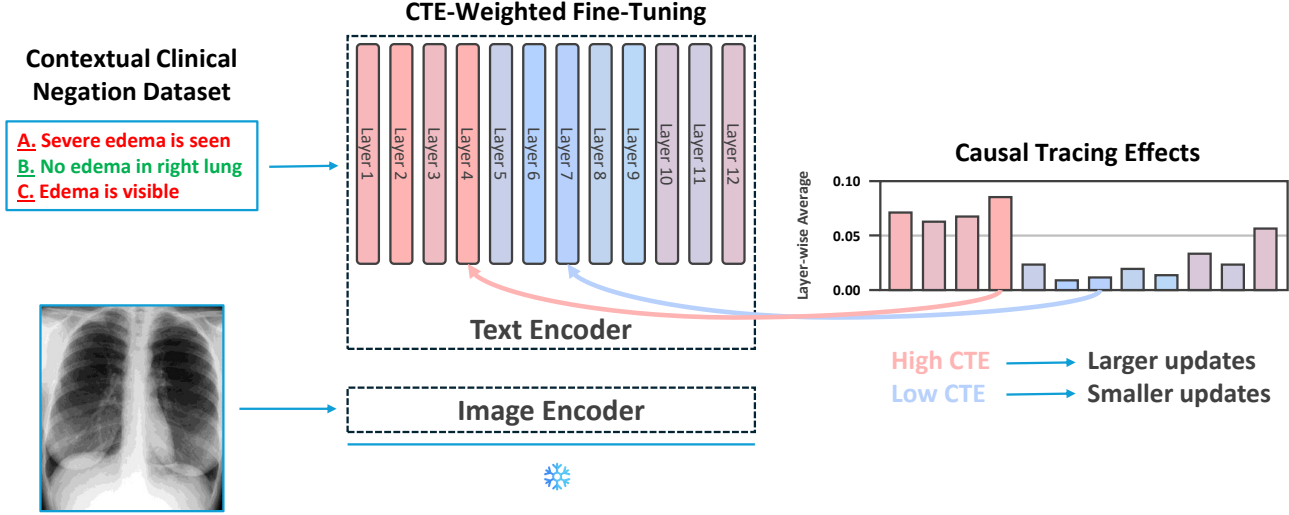


Figure 4. Overview of Negation-Aware Selective Training (NAST). Layer-wise causal tracing estimates each text encoder layer’s contribution to negation processing. The resulting CTE scores guide fine-tuning on the contextual negation dataset via layer-specific gradient scaling, assigning larger updates to high-CTE layers and smaller updates to low-CTE layers.

Structured Clinical Facts. Each study provides disease-level annotations specifying condition, existence, location, and severity. We convert these into canonical structured facts,

(condition, existence, location, severity),

retaining only definitive labels and excluding uncertain cases.

Contextual Negation Construction. From each true fact, we generate *contextual negations* by minimally altering exactly one attribute while keeping others fixed. We consider three types: existence (present vs. absent), location (e.g., left vs. right), and severity (e.g., small vs. large). These controlled perturbations yield clinically plausible, fine-grained counterfactuals.

Caption Generation and Formats. All facts are verbalized into radiology-style statements. We create two supervision formats: (i) *claim-based contrast sets* with one true claim and multiple hard negatives, and (ii) *single negated captions* for auxiliary contrastive training.

This process produces approximately one million image–text pairs, which we partition into training, validation, and test splits at the patient level to prevent data leakage. Compared to open-domain negation datasets (Alhamoud et al., 2025; Singh et al., 2024), our scale is sufficient due to the restricted ontology, precise annotations, and targeted counterfactual supervision. Additional details are provided in Appendix C.

4.2. Estimating Layer-Wise Causal Contribution to Negation

Our framework derives layer-wise importance weights to modulate gradient updates during fine-tuning, targeting layers based on their contribution to negation processing. This design minimizes changes to less relevant layers, preserving pretrained capabilities. We adopt a causal tracing approach (Meng et al., 2023), inspired by (Quantmeyer et al., 2024a), and adapt it to the medical imaging domain and our training objective.

Causal Probing Data. We construct a causal probing set from CAD annotations with high certainty and severe disease labels. For each condition, we generate paired captions: a *correct* caption describing the true clinical state (presence or absence) and a corresponding *foil* caption describing the opposite state, constrained to have identical token lengths. Unlike prior work that uses vague quantifiers such as “some” (Quantmeyer et al., 2024a), we introduce the modifier “severe” for affirmative findings (e.g., “severe edema” vs. “no edema”), yielding a clearer semantic contrast in the medical setting.

Causal Tracing in CLIP. Given an image–caption pair, we compute CLIP similarity scores for the correct and foil captions, denoted S^{corr} and S^{foil} , and define $d = S^{\text{corr}} - S^{\text{foil}}$ as the baseline negation sensitivity.

We record text-encoder hidden states from the foil forward pass. In a second pass with the correct caption, we intervene by replacing the hidden state at layer ℓ and token position p with the corresponding foil representation, producing an intervened score $S^{\ell,p}$. Following (Quantmeyer et al., 2024a),

we compute

$$d^{\ell,p} = S^{\text{corr}} - S^{\ell,p}, \quad \text{CTE}(\ell, p) = \frac{d^{\ell,p}}{d}.$$

$\text{CTE}(\ell, p)$ quantifies the fraction of negation-sensitive signal attributable to position (ℓ, p) .

As shown in Figure 5, negation-sensitive signals are concentrated in early layers (1–4), rather than uniformly distributed, indicating that negation processing emerges at specific stages of the CLIP text encoder. Additional details are provided in Appendix D.

4.3. CTE-Weighted Layer-Specific Adaptation

We leverage the layer-wise causal tracing effects (CTEs) estimated in the previous subsection to guide selective fine-tuning of CLIP-based medical VLMs. To achieve parameter-efficient adaptation, we fine-tune the model using Low-Rank Adaptation (LoRA) (Hu et al., 2022) modules inserted into the transformer layers, while keeping the backbone weights frozen.

From CTE to Training Weights. Let CTE_ℓ denote the aggregated causal tracing effect of layer ℓ , obtained by averaging token-level CTE scores over negation-bearing tokens and samples (see Appendix D for details). To ensure stable optimization, we normalize these scores across layers using min–max normalization,

$$\alpha_\ell = \frac{\text{CTE}_\ell - \min_k \text{CTE}_k}{\max_k \text{CTE}_k - \min_k \text{CTE}_k},$$

where k indexes all layers of the text encoder. This yields layer weights $\alpha_\ell \in [0, 1]$. Bounding the weights prevents excessively large updates and avoids disrupting the learning dynamics. We retain a global learning rate and treat α_ℓ as a relative modulation factor rather than a replacement for standard optimization hyperparameters.

CTE-Weighted Gradient Updates. Let g_ℓ denote the gradient of the LoRA parameters at layer ℓ . During fine-tuning, we apply CTE-aware scaling to obtain

$$\tilde{g}_\ell = \alpha_\ell^\beta \cdot g_\ell,$$

where $\beta > 0$ is a sharpness hyperparameter controlling how strongly updates are concentrated on high-CTE layers relative to low-CTE layers. Larger values of β accentuate differences between layers with high and low causal contribution, while smaller values smooth updates across layers. The optimizer then proceeds using \tilde{g}_ℓ with the original learning rate, effectively inducing layer-specific learning rates grounded in causal interpretability.

Training Objectives. We fine-tune the model using two types of negation-enriched supervision.

Single-caption negation supervision. For image–caption pairs containing explicit negation, we adopt the standard CLIP contrastive objective. Given a batch $\mathcal{B}_{\text{cap}} = \{(I_i, T_i)\}_{i=1}^N$, we compute the i -th image–text similarity matrix and apply the symmetric contrastive loss $\mathcal{L}_{\text{CLIP}}(\mathcal{B}_{\text{cap}})$, encouraging high similarity for matched pairs and low similarity for mismatches.

Claim-based caption supervision. For samples paired with a set of K mutually exclusive claims $\{T_{i,1}, \dots, T_{i,K}\}$ (with exactly one correct claim), we compute cosine similarities between the image I_i and each claim caption as logits $\{\ell_{i,1}, \dots, \ell_{i,K}\}$. We then apply a claim-ranking loss,

$$\mathcal{L}_{\text{claim}} = \frac{1}{M} \sum_{i=1}^M \log \frac{\exp(\ell_{i,c_i})}{\sum_{j=1}^K \exp(\ell_{i,j})},$$

where M denotes the number of image–claim sets in the batch and c_i denotes the index of the correct claim for image i . This objective encourages the model to assign higher similarity to the semantically correct claim than to closely matched negated or affirmative alternatives.

Combined Objective. The final training loss is a weighted combination of the two objectives,

$$\mathcal{L}_{\text{total}} = \lambda \mathcal{L}_{\text{CLIP}} + (1 - \lambda) \mathcal{L}_{\text{claim}},$$

with all gradients modulated by the CTE-based scaling described above. This approach integrates causal interpretability directly into the optimization process, focusing adaptation on layers that are causally responsible for negation understanding while preserving overall multimodal alignment.

5. Experiments and Results

We evaluate whether Negation-Aware Selective Fine-Tuning (NAST) improves negation understanding in vision–language models while remaining parameter-efficient and preserving performance on tasks related to standard (non-negated) language.

5.1. Experimental Setup

We compare our approach to CLIP (Radford et al., 2021) and three representative negation-aware variants: NegCLIP (Yuksekgonul et al., 2022), ConCLIP (Singh et al., 2024), and the negation-focused CLIP model, presented by Alhamoud et al. (2025). All models are initialized from their publicly released pretrained checkpoints. Baseline methods are evaluated directly using their original pretrained weights. Fine-tuning of our method is performed via LoRA-based

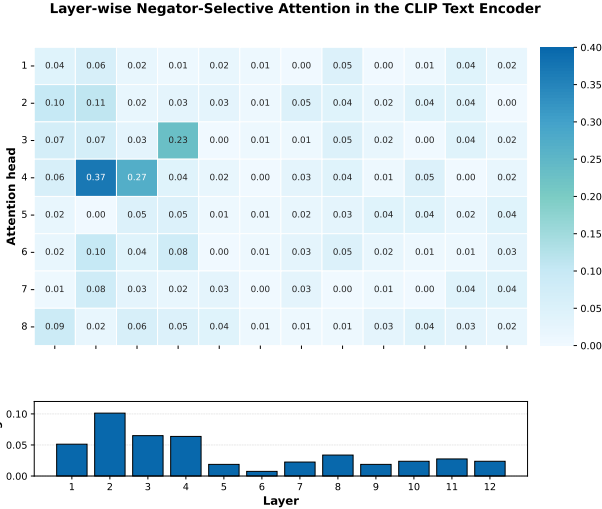


Figure 5. Negator-selective attention across layers and heads in the CLIP text encoder. The heatmap shows negator-selective attention per head, and the bar plot shows layer-wise averages. Negation-sensitive attention concentrates in early layers (1–4), peaking at layer 2, indicating localized rather than uniformly distributed processing.

adapters, keeping the backbone frozen to enable parameter-efficient adaptation. Optimization uses AdamW (Loshchilov & Hutter, 2017) with a fixed learning rate, and all experiments are conducted on a single NVIDIA RTX 4070 GPU.

5.2. Evaluation Protocol

Evaluation is conducted on the test split of the contextual negation benchmark (Section 4.1) under two settings: (i) single-caption image–text matching and (ii) claim-based caption sets, where multiple clinically plausible descriptions compete for each image. Models compute cosine similarity between image and text embeddings. In the single-caption setting, performance is measured by retrieval accuracy (the proportion of images for which the correct caption ranks highest). In the claim-based setting, accuracy reflects how often the correct clinical description receives the highest similarity score. This protocol evaluates the model’s ability to distinguish fine-grained affirmative and negated statements.

5.3. Main Results on Contextual Negation Tasks

For retrieval, models compute cosine similarity between image and caption embeddings, and performance is measured using Recall@1 (R@1) and Recall@5 (R@5). For claim-based evaluation, each image is paired with K clinically plausible descriptions (typically $K \in [5, 7]$), exactly one correct; accuracy is the proportion of samples where the correct claim is ranked highest.

Table 1 reports the results. Across both tasks, NAST consis-

Table 1. Main results on contextual negation tasks (%).

Model	R@1 ↑	R@5 ↑	Claim Acc. ↑
CLIP	23.5	34.7	24.6
NegCLIP	36.2	52.4	41.3
ConCLIP	39.7	55.8	44.9
NegBench	43.1	59.2	48.7
NAST (Ours)	49.5	65.7	55.6

Table 2. Performance on affirmative-only (non-negated) captions (%).

Model	R@1 ↑	R@5 ↑	Claim Acc. ↑
CLIP	41.8	58.6	46.2
NegCLIP	49.7	66.3	54.1
ConCLIP	51.2	68.0	55.6
NegBench	53.8	70.4	58.9
NAST (Ours)	54.6	71.2	59.8

tently outperforms other baselines. Among negation-aware methods, NegBench (Alhamoud et al., 2025) performs better than ConCLIP (Singh et al., 2024), which in turn outperforms NegCLIP (Yuksekgonul et al., 2022). These findings suggest that while negation-focused pretraining improves over standard CLIP, substantial limitations remain in handling contextual clinical negation.

Notably, the relative gains of NAST are larger in the claim-based setting than in retrieval, indicating that CTE-weighted updates particularly enhance fine-grained polarity discrimination rather than merely improving global image–text alignment.

5.4. Performance on Non-Negated Captions

To verify that improvements in negation sensitivity do not come at the expense of general vision–language alignment, we evaluate all models on the *affirmative-only* subset of the contextual benchmark. This subset contains single-caption and claim-based samples that do not include explicit negation cues, allowing us to assess whether NAST preserves performance on standard descriptive statements.

Table 2 shows that NAST maintains competitive performance on non-negated captions. Compared to its pretrained counterpart, the model exhibits better performance, indicating that CTE-weighted adaptation selectively improves negation understanding without degrading overall alignment. Importantly, NAST does not overfit to negation patterns at the expense of affirmative reasoning.

Table 3. Affirmative–Negation performance gap (Claim Accuracy %). Lower is better.

Model	Gap (Affirmative – Negation)
CLIP	21.6
NegCLIP	12.8
ConCLIP	10.7
NegBench	10.2
NAST (Ours)	4.2

5.5. Reduction of Affirmative–Negation Performance Gap

To directly quantify improvements in polarity sensitivity, we measure the performance gap between affirmative and negated samples for each model. For both retrieval and claim-based tasks, we compute the difference between performance on the affirmative-only subset and the negated one. A smaller gap indicates better robustness to negation.

Table 3 reports the gap values for claim-based accuracy. Standard CLIP exhibits a substantial affirmative bias, with markedly higher performance on non-negated captions than on negated ones. Although negation-aware baselines reduce this gap to some extent, a noticeable disparity remains. In contrast, NAST narrows the affirmative–negation gap much further, demonstrating improved polarity sensitivity without sacrificing affirmative performance.

Importantly, NAST reduces the gap not by lowering affirmative performance, but by increasing accuracy on negated captions, indicating that the gains stem from improved negation understanding rather than global calibration shifts.

5.6. Impact of CTE-Weighted Updates on Learning Dynamics

We analyze how CTE-weighted adaptation influences optimization across layers. Since NAST scales gradients by estimated causal contribution to negation, we examine the distribution of update magnitudes during fine-tuning.

We compute the average ℓ_2 norm of parameter updates per layer under both uniform and CTE-weighted training. Uniform fine-tuning distributes updates relatively evenly across layers. In contrast, CTE-weighted training concentrates updates in layers identified as negation-sensitive, while reducing changes in less relevant layers.

Table 4 reports the proportion of total update magnitude allocated to the top- k negation-sensitive layers (by CTE score). The results show that CTE-weighted training significantly increases update concentration in these layers, confirming that it actively reshapes learning dynamics rather than merely re-scaling gradients.

Table 4. Proportion of total update magnitude allocated to top negation-sensitive layers (%).

Method	Top-3 Layers	Top-5 Layers
Uniform Fine-Tuning	28.4	41.7
NAST (CTE-Weighted)	52.6	69.3

Importantly, this concentration of updates correlates with improved negation performance without degrading affirmative alignment. This suggests that directing optimization toward causally relevant layers yields more efficient and targeted adaptation. These findings support our central hypothesis: mechanistic interpretability signals can be transformed into actionable training guidance that shapes the model’s negation handling in a principled manner.

6. Conclusion

We examined negation understanding in medical vision–language models and identified a systematic affirmative bias under polarity-controlled descriptions. To diagnose this issue, we introduced a radiology-specific benchmark that isolates negation effects. We then proposed Negation-Aware Selective Training (NAST), an interpretability-guided fine-tuning strategy that uses layer-wise causal tracing to modulate gradient updates. NAST improves discrimination between affirmative and negated clinical statements while preserving overall vision–language alignment. These results demonstrate that causal interpretability can guide targeted adaptation in safety-critical multimodal systems.

Impact Statement

This work addresses a clinically critical limitation of medical vision–language models: their difficulty in interpreting negation. In radiology, negated findings (e.g., “no pneumothorax”) directly influence diagnostic reasoning and patient management. Improving negation sensitivity can therefore enhance the reliability of multimodal AI systems for report analysis, retrieval, and decision support.

However, our approach does not eliminate broader risks of medical AI deployment. The method is evaluated on structured datasets derived from MIMIC-CXR and may not generalize across institutions, modalities, or linguistic styles without further validation. Moreover, improved negation handling does not imply clinical readiness; such systems remain assistive tools requiring human oversight. We hope this work encourages further research on robust and interpretable multimodal models in safety-critical domains.

Acknowledgements

Our work was supported by NSF award 2443639, and NIH awards, P20GM103446, and U54GM104941.

References

Adiba, F. I. and Beheshti, R. Toward revealing nuanced biases in medical llms. *arXiv preprint arXiv:2507.21176*, 2025.

Adiba, F. I., Danduri, V., Piya, F. L., Abbasi, A., Gupta, M., and Beheshti, R. A multimodal data processing pipeline for mimic-iv dataset. *arXiv preprint arXiv:2601.11606*, 2026.

Alayrac, J.-B., Donahue, J., Luc, P., Miech, A., Barr, I., Hasson, Y., Lenc, K., Mensch, A., Millican, K., Reynolds, M., et al. Flamingo: a visual language model for few-shot learning. *Advances in neural information processing systems*, 35:23716–23736, 2022.

Alhamoud, K., Alshammari, S., Tian, Y., Li, G., Torr, P. H. S., Kim, Y., and Ghassemi, M. Vision-language models do not understand negation. In *Proceedings of the IEEE/CVF Conference on Computer Vision and Pattern Recognition (CVPR)*, pp. 29612–29622, 2025.

Bannur, S., Hyland, S., Liu, Q., Perez-Garcia, F., Ilse, M., Castro, D. C., Boecking, B., Sharma, H., Bouzid, K., Thieme, A., et al. Learning to exploit temporal structure for biomedical vision-language processing. In *Proceedings of the IEEE/CVF Conference on Computer Vision and Pattern Recognition*, pp. 15016–15027, 2023.

Buettner, K. and Kovashka, A. Investigating the role of attribute context in vision-language models for object recognition and detection. In *Proceedings of the IEEE/CVF Winter Conference on Applications of Computer Vision*, pp. 5474–5484, 2024.

Cai, Y., Thomason, J., and Rostami, M. Tng-clip: Training-time negation data generation for negation awareness of clip. *arXiv preprint arXiv:2505.18434*, 2025.

Chapman, W. W., Bridewell, W., Hanbury, P., Cooper, G. F., and Buchanan, B. G. A simple algorithm for identifying negated findings and diseases in discharge summaries. *Journal of biomedical informatics*, 34(5):301–310, 2001.

Daelemans, W. Conandoyle-neg: Annotation of negation in conan doyle stories. 2012.

Eslami, S., Meinel, C., and De Melo, G. Pubmedclip: How much does clip benefit visual question answering in the medical domain? In *Findings of the Association for Computational Linguistics: EACL 2023*, pp. 1181–1193, 2023.

Ettinger, A. What bert is not: Lessons from a new suite of psycholinguistic diagnostics for language models. *Transactions of the Association for Computational Linguistics*, 8:34–48, 2020.

Fayyaz, H., Poulain, R., and Beheshti, R. Enabling scalable evaluation of bias patterns in medical llms. *arXiv preprint arXiv:2410.14763*, 2024.

Han, H., Wang, A. J., Liu, F., and Zhu, J. Negation-aware test-time adaptation for vision-language models. *arXiv preprint arXiv:2507.19064*, 2025.

Harkema, H., Dowling, J. N., Thornblade, T., and Chapman, W. W. Context: an algorithm for determining negation, experiencer, and temporal status from clinical reports. *Journal of biomedical informatics*, 42(5):839–851, 2009.

Hosseini, A., Reddy, S., Bahdanau, D., Hjelm, R. D., Sorondi, A., and Courville, A. Understanding by understanding not: Modeling negation in language models. *arXiv preprint arXiv:2105.03519*, 2021.

Hu, E. J., Shen, Y., Wallis, P., Allen-Zhu, Z., Li, Y., Wang, S., Wang, L., Chen, W., et al. Lora: Low-rank adaptation of large language models. *ICLR*, 1(2):3, 2022.

Huang, S.-C., Shen, L., Lungren, M. P., and Yeung, S. Gloria: A multimodal global-local representation learning framework for label-efficient medical image recognition. In *Proceedings of the IEEE/CVF international conference on computer vision*, pp. 3942–3951, 2021.

Irvin, J., Rajpurkar, P., Ko, M., Yu, Y., Ciurea-Ilcus, S., Chute, C., Marklund, H., Haghgoor, B., Ball, R., Shpanskaya, K., et al. Chexpert: A large chest radiograph dataset with uncertainty labels and expert comparison. In *Proceedings of the AAAI conference on artificial intelligence*, volume 33, pp. 590–597, 2019.

Johnson, A. E. W., Pollard, T. J., Greenbaum, N. R., Lungren, M. P., Deng, C.-y., Peng, Y., Lu, Z., Mark, R. G., Berkowitz, S. J., and Horng, S. Mimic-cxr-jpg, a large publicly available database of labeled chest radiographs. *PhysioNet*, 2019.

Johnson, A. E. W., Lungren, M. P., Peng, Y., Lu, Z., Mark, R. G., Berkowitz, S. J., and Horng, S. Mimic-cxr-jpg: Chest radiographs with structured labels, 2024. URL <https://doi.org/10.13026/jsn5-t979>. RRID:SCR_007345.

Khattak, M. U., Kunhimon, S., Naseer, M., Khan, S., and Khan, F. S. Unimed-clip: Towards a unified image-text pretraining paradigm for diverse medical imaging modalities. *arXiv preprint arXiv:2412.10372*, 2024.

Ko, H. and Park, C.-M. Bringing clip to the clinic: Dynamic soft labels and negation-aware learning for medical analysis. In *Proceedings of the Computer Vision and Pattern Recognition Conference*, pp. 25897–25906, 2025.

Li, J., Li, D., Xiong, C., and Hoi, S. Blip: Bootstrapping language-image pre-training for unified vision-language understanding and generation. In *International conference on machine learning*, pp. 12888–12900. PMLR, 2022.

Lin, W., Zhao, Z., Zhang, X., Wu, C., Zhang, Y., Wang, Y., and Xie, W. Pmc-clip: Contrastive language-image pre-training using biomedical documents. In *International Conference on Medical Image Computing and Computer-Assisted Intervention*, pp. 525–536. Springer, 2023.

Liu, Z., Chen, Z., Liu, H., Luo, C., Tang, X., Wang, S., Zeng, J., Dai, Z., Shi, Z., Wei, T., et al. Seeing but not believing: Probing the disconnect between visual attention and answer correctness in vlms. *arXiv preprint arXiv:2510.17771*, 2025.

Loshchilov, I. and Hutter, F. Decoupled weight decay regularization. *arXiv preprint arXiv:1711.05101*, 2017.

Meng, K., Bau, D., Andonian, A., and Belinkov, Y. Locating and editing factual associations in gpt. *Transactions on Machine Learning Research*, 2023.

Moor, M., Huang, Q., Wu, S., Yasunaga, M., Dalmia, Y., Leskovec, J., Zakka, C., Reis, E. P., and Rajpurkar, P. Med-flamingo: a multimodal medical few-shot learner. In *Machine Learning for Health (ML4H)*, pp. 353–367. PMLR, 2023.

Poulain, R., Fayyaz, H., and Beheshti, R. Aligning (medical) llms for (counterfactual) fairness. *arXiv preprint arXiv:2408.12055*, 2024.

Quantmeyer, F., Schüler, N., and Frank, A. How does clip process negation? layer-wise and head-wise analysis of linguistic operators in vision-language models. *arXiv preprint arXiv:2401.05721*, 2024a.

Quantmeyer, V., Mosteiro, P., and Gatt, A. How and where does clip process negation? *arXiv preprint arXiv:2407.10488*, 2024b.

Radford, A., Kim, J. W., Hallacy, C., Ramesh, A., Goh, G., Agarwal, S., Sastry, G., Askell, A., Mishkin, P., Clark, J., Krueger, G., and Sutskever, I. Learning transferable visual models from natural language supervision. In *Proceedings of the 38th International Conference on Machine Learning (ICML)*, 2021.

Singh, J., Shrivastava, I., Vatsa, M., Singh, R., and Bharati, A. Learn “no” to say “yes” better: Improving vision-language models via negations. *arXiv preprint arXiv:2403.20312*, 2024.

Vatsa, M., Bharati, A., Mittal, S., and Singh, R. From no to know: Taxonomy, challenges, and opportunities for negation understanding in multimodal foundation models. *arXiv preprint arXiv:2502.09645*, 2025.

Wang, Z., Wu, Z., Agarwal, D., and Sun, J. Medclip: Contrastive learning from unpaired medical images and text. In *Proceedings of the Conference on Empirical Methods in Natural Language Processing. Conference on Empirical Methods in Natural Language Processing*, volume 2022, pp. 3876, 2022.

Wei, X., Kurtz, C., and Cloppet, F. Qwenclip: Boosting medical vision-language pretraining via llm embeddings and prompt tuning. *arXiv preprint arXiv:2511.13876*, 2025.

Yuksekgonul, M., Bianchi, F., Kalluri, P., Jurafsky, D., and Zou, J. When and why vision-language models behave like bags-of-words, and what to do about it? *arXiv preprint arXiv:2210.01936*, 2022.

Zhang, M., Hu, X., Gu, L., Harada, T., Kobayashi, K., Summers, R. M., and Zhu, Y. Cad-chest: Comprehensive annotation of diseases based on mimic-cxr radiology report, 2023a. URL <https://doi.org/10.13026/44pd-vz36>. RRID:SCR_007345.

Zhang, S., Xu, Y., Usuyama, N., Xu, H., Bagga, J., Tinn, R., Preston, S., Rao, R., Wei, M., Valluri, N., et al. Biomed-clip: a multimodal biomedical foundation model pre-trained from fifteen million scientific image-text pairs. *arXiv preprint arXiv:2303.00915*, 2023b.

Zhang, Y., Jiang, H., Miura, Y., Manning, C. D., and Langlotz, C. P. Contrastive learning of medical visual representations from paired images and text. In *Machine learning for healthcare conference*, pp. 2–25. PMLR, 2022.

A. Affirmative Alternatives for Absent Conditions

To enable controlled comparison between negated and affirmative-equivalent clinical descriptions, we curate a set of affirmative alternatives corresponding to the absence (label = 0) of each CheXpert condition. Each alternative expresses the same underlying clinical state as its negated counterpart while avoiding explicit negation cues (e.g., “no”, “without”). All mappings were developed in consultation with a board-certified radiologist to ensure clinical validity, mutual exclusivity, and consistency with standard radiology reporting conventions.

For conditions labeled as present (label = 1), we retain the canonical CheXpert condition names when generating MCQ answer choices. Two minor modifications are introduced for clarity and clinical naturalness: we use “pulmonary edema” instead of “edema”, and “pleural abnormality” instead of “Pleural Other”.

Table 5 lists the affirmative alternatives used throughout the benchmark.

Condition (Absent)	Affirmative Alternative Description
Atelectasis	well-aerated expanded lungs
Cardiomegaly	normal heart size
Consolidation	clear lung parenchyma
Edema	normal pulmonary vascularity
Enlarged Cardiomediastinum	normal mediastinal contours
Fracture	intact bony structures
Lung Lesion	homogeneous lung parenchyma
Lung Opacity	well-aerated lung fields
Pleural Effusion	sharp costophrenic angles
Pleural Other	smooth pleural surfaces
Pneumonia	aerated alveoli
Pneumothorax	fully expanded lungs
Support Devices	device-free chest

Table 5. Affirmative alternatives used to replace negated clinical findings (label = 0) in the benchmark.

B. Full Benchmark Construction Details and Prompts

This section provides the complete benchmark construction procedure, including label configuration generation, negated MCQ synthesis, affirmative-equivalent rewriting, and stored metadata fields.

Raw Choice Generation. For each filtered CheXpert study (Section X), we randomly sample three conditions annotated as present or absent. The ground-truth binary configuration forms the correct answer choice. We then generate three contrastive configurations by permuting the binary labels, yielding four candidate options per sample. These configurations define the semantic content of the multiple-choice question and enable controlled comparison between correct and incorrect clinical states.

Lung Lesion = 0, Cardiomegaly = 0, Pneumothorax = 1
Lung Lesion = 0, Cardiomegaly = 0, Pneumothorax = 0
Lung Lesion = 1, Cardiomegaly = 1, Pneumothorax = 1
Lung Lesion = 1, Cardiomegaly = 0, Pneumothorax = 1

Negated MCQ Generation. Given the raw label configurations and standardized condition names (Appendix A), we prompt GPT-5.1 to generate a radiology-style multiple-choice question containing explicit negation. The model is constrained to preserve the specified clinical facts while varying only surface realization. The complete prompt template is provided below.

You are a radiologist creating a multiple-choice question based on chest radiograph findings.

Task:

- Write a clear and neutral question stem that asks which option correctly describes the image findings. Keep the question generic, without revealing information about

what is or isn't present.

- Rephrase each option into natural medical language and radiology report summary.
- For conditions marked =1, use varied ways to express presence, e.g.
"with Cardiomegaly", "showing Cardiomegaly", "evidence of Cardiomegaly",
"Cardiomegaly noted".
- For conditions marked =0, use varied ways to express absence, e.g.
"without Edema", "no Edema", "Edema absent", "free of Edema", "lacking Edema".
- Use natural conjunctions and negations, with patterns like:
"A and B without C", "A, B, but not C",
"C absent while A and B present",
"No C, with A and B",
"A noted, no sign of B or C".
- State ONLY the presence or absence of the specified conditions,
and avoid explanatory phrases or redundant descriptions.
- Output only the question and its options (A{D}), with no explanations or extra text.

Condition names to use (USE THESE EXACT TERMS ONLY):
{relevant_map}

Ground truth values:
{raw_choices}

This prompt yields a natural radiology-style question and four answer options, for example:

Which of the following radiology report summaries best describes the findings on this chest radiograph?

- A. Pneumothorax present, with no cardiomegaly and atelectasis absent.
- B. Atelectasis noted, without cardiomegaly or pneumothorax.
- C. No cardiomegaly, free of atelectasis, and lacking pneumothorax.
- D. Cardiomegaly evident, with no atelectasis or pneumothorax.

Affirmative-Equivalent Rewriting. To isolate linguistic polarity while preserving semantic equivalence, we generate an affirmative-equivalent version of each MCQ. The negated question and answer options, together with the predefined affirmative mapping (Appendix A), are provided to GPT-5.1 with strict instructions to modify only negation-bearing phrases. The rewriting process preserves sentence structure and content, ensuring that the resulting MCQ differs from the original solely in polarity expression.

You are rewriting radiology multiple-choice options to replace ONLY the negation phrases with affirmative alternatives.

Task:

- Keep the overall sentence structure, word order, and style as close as possible to the original.
- ONLY change phrases that negate a condition (e.g., "no X", "without X", "X absent", "free of X", "lacking X", "no evidence of X", "no radiographic evidence of X").
- Replace negation phrases with the affirmative alternative provided below.
- Make MINIMAL grammatical adjustments ONLY when necessary.
- For conditions that are present (=1), keep the EXACT original wording unchanged.
- Ensure the result is grammatically correct and sounds natural.
- If a negation phrase includes words like "while", "and", or "with", adjust minimally to maintain natural grammar.
- If replacing a negated abnormality (=0) with a normal/benign affirmative finding, remove or replace adversative conjunctions (e.g., "but", "however") when needed.
- If replacing a negation results in repeated "with" constructions, replace the later "with" with "and" when it improves fluency.

Output format:

- A. [rewritten option A]
- B. [rewritten option B]
- C. [rewritten option C]
- D. [rewritten option D]

Do NOT include the question stem, explanations, or extra text.

Affirmative replacements for absent conditions (=0):
 {rewrite_map}

Options to rewrite:
 {options_text}

Ground truth (1=present, 0=absent):
 {raw_choices}

Applying this prompt yields an affirmative-equivalent MCQ that is identical to the negated version except for polarity-related phrases:

Which of the following radiology report summaries best describes the findings on this chest radiograph?
 A. Pneumothorax present, with normal heart size and well-aerated expanded lungs.
 B. Atelectasis noted, with normal heart size and fully expanded lungs.
 C. Normal heart size, with well-aerated expanded lungs and fully expanded lungs.
 D. Cardiomegaly evident, with well-aerated expanded lungs and fully expanded lungs.

Stored Benchmark Fields. For each sample, we store the subject ID, study ID, question stem, raw binary label configurations, the four negated MCQ options, the four affirmative-equivalent options, and the index of the correct answer. Although CLIP-style models operate directly on image–text pairs, we retain the question stem to support evaluation of VLMs that accept question–image inputs (e.g., instruction-following multimodal models), ensuring broader applicability of the benchmark.

C. Fine-Tuning Dataset Construction Details

This section describes the dataset construction pipeline used for contextual negation fine-tuning, including caption realization, prompt design, validation, and dataset composition.

Language Model for Caption Realization. Captions are generated using an instruction-tuned LLaMA 3.1 8B model. The model is used strictly for surface realization: all semantic content is deterministically derived from structured CAD annotations. Prompts explicitly constrain the model from introducing new findings, locations, or severity descriptors, ensuring faithful verbalization of the underlying clinical facts.

Prompt Templates. We employ structured prompts that take filled-in clinical facts as input and request concise radiology-style sentences. An example template is shown below.

Instruction:
 Generate a concise radiology-style sentence from the structured fact below.
 Do not introduce new findings, locations, or severity descriptors.

Fact:
 Condition: Pleural effusion
 Existence: Absent
 Location: Right
 Severity: None

For claim-based contrast sets, multiple facts are provided in a single prompt and the model is instructed to generate one sentence per fact, preserving order.

Automatic Validation. Generated captions are retained only if they satisfy three criteria: (i) explicit mention of the specified condition, (ii) correct expression of the targeted attribute (existence, location, or severity), and (iii) absence of unsupported medical terminology. Captions failing any criterion are discarded and regenerated.

Example Samples. **Existence Negation (Single Caption):** Image: CXR Caption: “*There is no pulmonary edema.*”

Location Negation (Claim-Based Set):

- True: “*There is consolidation in the right lower lobe.*”
- False: “*There is consolidation in the left lower lobe.*”
- False: “*There is no consolidation.*”

Severity Negation (Claim-Based Set):

- True: “*There is a small left pneumothorax.*”
- False: “*There is a large left pneumothorax.*”
- False: “*There is no pneumothorax.*”

Dataset Composition. The final dataset comprises both claim-based contrast sets and single-caption negation examples, balanced across conditions and negation types. This design ensures broad coverage while maintaining high per-sample supervision quality.

D. Construction of Causal Tracing Inputs

This section describes the construction of inputs used for causal tracing analyses to localize negation-sensitive components within the CLIP text encoder.

D.1. Data Selection

We derive causal tracing inputs from the CAD-Chest dataset (Zhang et al., 2023a), which provides comprehensive disease annotations for chest radiographs in the MIMIC-CXR-JPG collection (Johnson et al., 2024). To ensure unambiguous polarity contrasts, we restrict attention to cases annotated with `level = severe` and high certainty, where

$$\text{probability_score} \in \{-3, 3\}.$$

Here, -3 denotes confident absence and 3 confident presence. This filtering ensures that polarity differences reflect clear semantic distinctions rather than uncertainty.

D.2. Paired Caption Construction

For each disease finding, we construct paired captions that differ only in polarity:

- **Affirmative:** “There is severe *[disease]*.”
- **Negated:** “There is no *[disease]*.”

Including the modifier “severe” approximately matches token length and syntactic complexity between variants, reducing confounds due to trivial lexical differences and following (Quantmeyer et al., 2024b).

We include both configurations encountered in MedNega-CXR: (i) cases where negation appears in the caption (`probability_score = -3`), and (ii) cases where negation appears in the foil option (`probability_score = 3`). This design captures negation processing regardless of whether polarity is expressed in the correct answer or its contrastive alternative.

D.3. Aggregation Across Negation Contexts

Because negation may appear in either the primary caption or the foil, we merge both subsets to obtain a unified characterization of negation-sensitive layers and positions. Aggregating across these contexts yields a comprehensive view of how negation information is encoded and propagated within the text encoder.

In total, this procedure yields $N = [\text{number}]$ paired instances spanning $[\text{number}]$ unique disease findings. These instances form the basis of the causal tracing analyses reported in Section 4 and guide the layer selection used in Negation-Aware Selective Training (NAST).